

Thermal sensor based on si single crystal implanted with different parties P⁺ and B⁺ ions

I. R. Bekpulatov*, Sh. K. Saliyeva, Z. R. Saidakhmedova, and D. T. Rasulova

Tashkent State Technical University, Tashkent, Uzbekistan

Abstract. The characteristics of existing temperature sensors based on silicon monocrystals are analyzed, and the reasons for the limited upper limit of temperature measurement are established. To increase sensitivity, expand the range of measured temperatures, and obtain a linear output characteristic of the temperature sensor, the authors propose to carry out phased implantation of P⁺ and B⁺ ions with decreasing energy in different directions of the Si(111) crystal followed by brief thermal, laser or IR radiation after each stage ion implantation. The distribution profiles of P and B atoms implanted into Si with a gradual decrease in energy are studied. The effect of subsequent thermal and IR annealing on the atomic distribution profiles and the characteristics of a thermal sensor was investigated.

A *p-i-n* diode with a high concentration of electrically active atoms ($N_p=10^{21} \text{ cm}^{-3}$, $N_B=2 \cdot 10^{21} \text{ cm}^{-3}$), with almost a step distribution of P and B atoms and a sharp boundary *p-i* and *i-n* was created areas with a high thermal sensitivity of 2.3 mV/K in a wide temperature range of 20-550 K.

1 Introduction

The particular sensitivity of the properties of semiconductor materials to the presence of minor impurities, temperature, pressure, exposure to electromagnetic radiation, etc. widely used to create various types of sensors [1-3]. Temperature-sensitive elements based on silicon were obtained in some works [3-6]. In particular, studies of the electrophysical properties of silicon diffusion-doped with manganese have shown [6] the possibility of obtaining a material with high thermal sensitivity. However, both in [6] and in other works [7-9] known to us about temperature sensors based on silicon, structures were obtained that can measure the temperature of objects only up to 350-380 K. This is because at these temperatures the impurity atoms ionize and at higher temperatures the silicon's own conductivity occurs. Another disadvantage of Si-based thermoelements is the non-linearity of their temperature response.

The work aims to develop a highly sensitive temperature sensor based on a Si(111) single crystal with a linear output characteristic in a wide temperature range. To this end, to create a silicon-based temperature sensor capable of measuring higher temperatures, we chose *p-i-n* structures.

The following technological methods are commonly used to create *p-i-n* structures:

* Corresponding author: bekpulatov85@rambler.ru

epitaxial-diffusion, two-sided-epitaxial and two-sided-diffusion methods [10].

In the manufacture of semiconductor devices, depending on the type of dopant and technology used, various defects are formed in the structures, which deteriorate the quality of the diodes and their breakdown characteristics. In addition, when using high-temperature technologies, such as epitaxial and diffusion technologies for creating pin-structures, it is possible to activate impurities of the source material, for example, Na atoms, which can create fast states, various traps [11], macroscopic fluctuations leading to the appearance of density tails [12], or large inhomogeneities, at least at high concentrations of about 10^{13} cm^{-2} [13, 14]. If they become possible tunneling, it is also possible for thermal excitation to the edge of mobility.

Therefore, to obtain the *p-i-n* structure, we chose the ion implantation method, which does not subject the sample to high-temperature heating. Our task was to create a thermal sensor that meets the following requirements:

- 1) small size;
- 2) high-temperature sensitivity;
- 3) a wide range of measured temperatures;
- 4) linearity of the temperature characteristics of the output signal of the sensor.

The last requirement was associated with the need to use the sensor as a primary device in the system for automatic control of the temperature of technological processes. Fulfillment of this requirement provided the sensor versatility for use in various technological processes.

2 Methods

To obtain a sensor that meets the above requirements, it was necessary to ensure the maximum degree of doping of the *p*- and *n*- layers and create sharp boundaries of the *p-i* and *i-n* – transitions. To obtain such abrupt transitions, we carried out the implantation of P^+ and B^+ ions in different directions of purified Si(111) single crystals. The experiments were carried out with samples of Si (111) *p*-type with a specific resistance of $\rho=3000$ and $6000 \text{ }\Omega\text{-cm}$, with a thickness of 0.1 to 1 mm. Moreover, the best characteristics were obtained using Si samples with a thickness of 0.1 mm.

Before ion implantation, the initial Si(111) samples were thoroughly cleaned by thermal heating in two stages: long at 1200 K and briefly at $T=1500 \text{ K}$, as well as a new method for vacuum cleaning of the Si surface developed by the authors [15], which is created in the near-surface the area of the gettering layer is implanted with Ba ions or low energy alkaline elements (up to 5 keV) and the subsequent removal of the getter layer by short-term high-temperature heating. The experiments were carried out in an ultrahigh-vacuum instrument with a three-mesh spherical energy analyzer with a retarding field, which allows the state of the film surface to be investigated using methods such as Auger electron spectroscopy (AES), characteristic energy loss spectroscopy (CELS), photoelectron spectroscopy (PES), and fast electron diffraction (FED), an also carry out various technological operations: thermal heating, electron bombardment, ion etching of the surface, laser annealing, ion implantation. The residual gas pressure in the instrument did not exceed 10^{-7} Pa . The implantation of P^+ and B^+ ions was carried out on a standard "Ion" type installation in a vacuum of 10^{-5} Pa at room temperature of the target. To create *p* and *n* layers in silicon, implantation of P^+ and B^+ ions was carried out, and subsequent annealing. The depth distribution profiles of the P and B atoms are calculated by quantitative Auger electron spectroscopy considering the elemental Auger sensitivity coefficients with matrix corrections [16]. In this case, layer-by-layer etching was carried out with Ar^+ ions with an energy of 1.5 keV falling at an angle of 15° to the surface. The etching rate was 3-4 Å/min.

3 Results and Discussion

Figure 1 shows the distribution profiles of boron atoms implanted in Si(111) with an energy $E_0=1$ keV and subjected to subsequent thermal and laser annealing.

Thermal annealing at $T = 900$ K of Si(111) samples implanted with B^+ ions with $E_0=1$ keV allows you to remove defects and to obtain in the sample of a sample ~ 40 Å single crystal film of boron silicide SiB_3 (Fig. 1). Pulsed laser annealing of Si(111) implanted with B^+ ions at $W=1.0$ J·cm $^{-2}$ allows one to obtain a heterostructural transition SiB_3 -Si with a sharper interface.

Thermal heating at $T = 1200$ K or laser annealing with $W=3$ J·cm $^{-2}$ is necessary for decomposing the chemical compound SiB_3 and the complete electrical activation of the remaining B^+ atoms. Note that after laser annealing of ion-implanted samples, an $n^- - p$ transition is formed in the case of P and $p^{++} - p$ - in the case of B. In addition, we also investigated the distribution profiles of the P and B atoms implanted in Si(111) with a higher energy of 10, 20 and 80 keV. In this case, ion-implanted samples were annealed by thermal heating and pulsed infrared (IR) radiation with a wavelength $\lambda=1$ μm and a pulse duration of \sim units of microseconds.

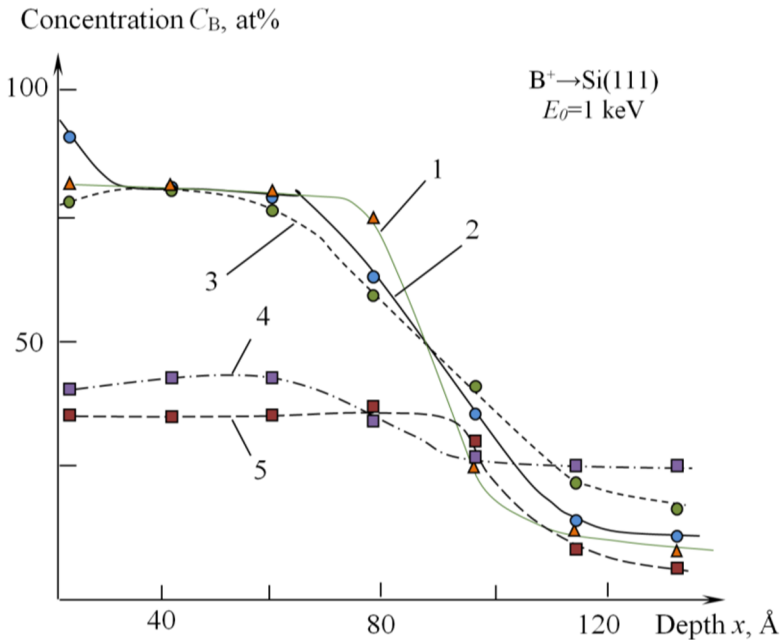


Fig. 1. Concentration distribution profiles of boron atoms implanted into Si(111) with energy $E_0 = 1$ keV over depth x , obtained after thermal annealing at (1) 300, (2) 900, and (3) 1200 K and laser annealing at energy density W of (4) 1.0 and (5) 3 J·cm $^{-2}$.

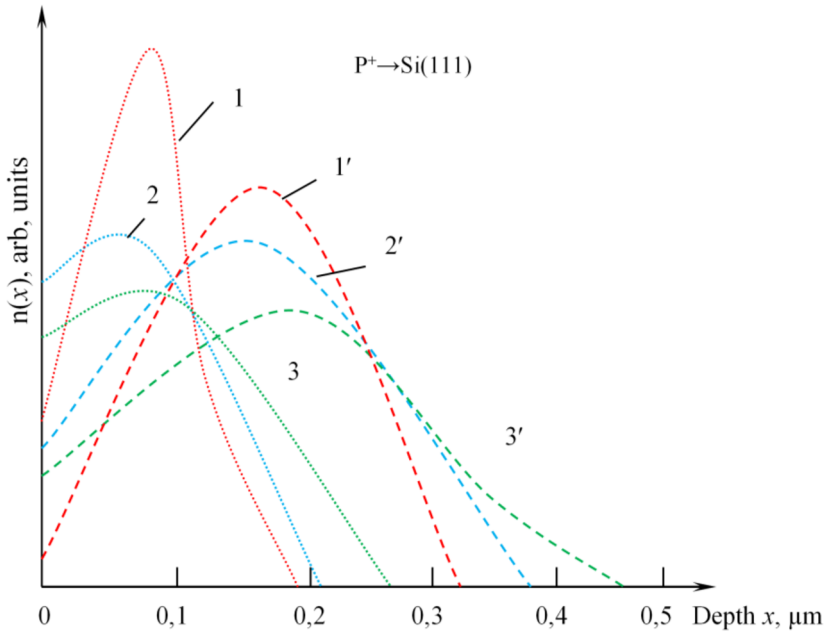


Fig. 2. Distribution profiles of P atoms implanted in Si(111) with $E_0 = 20$ keV (1), after IR annealing (2), thermal annealing at $T = 1200$ K (3), and with $E_0 = 80$ keV (1'), after IR annealing (2') and thermal annealing at $T = 1200$ K (3').

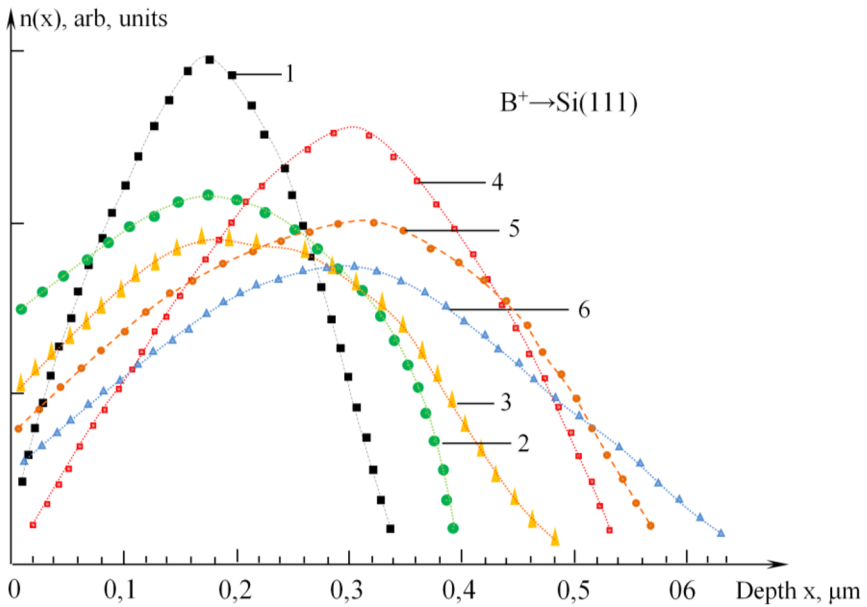


Fig. 3. Distribution profiles of B atoms implanted in Si(111) with $E_0 = 20$ keV (1), after IR annealing (2) or thermal annealing at $T = 1100$ K (3) and with $E_0 = 80$ keV (4), after IR annealing (5), thermal annealing at $T = 1100$ K (6).

Figures 2 and 3 show how the distribution profiles of implanted P and B atoms with different energies are transformed due to thermal and IR (infrared) annealing. As seen from

the above figures, annealing by infrared radiation and laser annealing, allows one to obtain sharper profiles of implanted atoms than thermal annealing.

Our earlier studies of the behavior of P and B atoms implanted in Si(111) with low energy (<5 keV) and high dose ($D \geq 10^{17} \text{ cm}^{-2}$) showed that most of the implanted atoms enter into a chemical compound with silicon atoms. The subsequent short-term thermal annealing at $T=900 \text{ K}$ leads to the formation of silicon phosphide and boron silicide [17].

It is obvious that at ion energies of the order of tens of keV at large irradiation doses, the concentration of impurity atoms is much less than that of Si atoms. However, this does not mean chemical interaction between atoms is impossible. Based on the analysis of the distribution profiles of P and B atoms implanted with a high dose of $D \approx 10^{17} \text{ cm}^{-2}$ with different energies before and after annealing with IR radiation, we determined the optimal energies, irradiation doses, and conditions of the subsequent annealing to obtain the maximum possible concentration of electrically active impurities P and B with their uniform distribution over the depth of the sample. It was found that to obtain a uniform distribution of P atoms in Si(111), it is necessary to conduct the implantation of P^+ ions first with the energy of $E_0=80 \text{ keV}$ and a dose of $D=1.8 \cdot 10^{16} \text{ cm}^{-2}$ (Fig.4), and then with $E_0=20 \text{ keV}$ and $D=1.8 \cdot 10^{15} \text{ cm}^{-2}$. Annealing with infrared radiation should be carried out after each ion implantation stage.

In the case of boron, we found that the optimal conditions for implantation and annealing are the following: first, implantation of B^+ ions $E_0=80 \text{ keV}$ and $D=0.9 \cdot 10^{16} \text{ cm}^{-2}$, then with $E_0=20 \text{ keV}$ and $D=3 \cdot 10^{15} \text{ cm}^{-2}$ and finally with $E_0=10 \text{ keV}$ and $D=1.8 \cdot 10^{15} \text{ cm}^{-2}$, annealing with infrared radiation should also be carried out after each stage of ion implantation (Fig. 5).

As can be seen from the above figures 4 and 5, carrying out ion implantation and subsequent annealing in the manner described above makes it possible to obtain an almost uniform distribution of P atoms in a layer $x \approx 0.4 \text{ }\mu\text{m}$ thick and B atoms in a layer with $x \approx 0.6 \text{ }\mu\text{m}$.

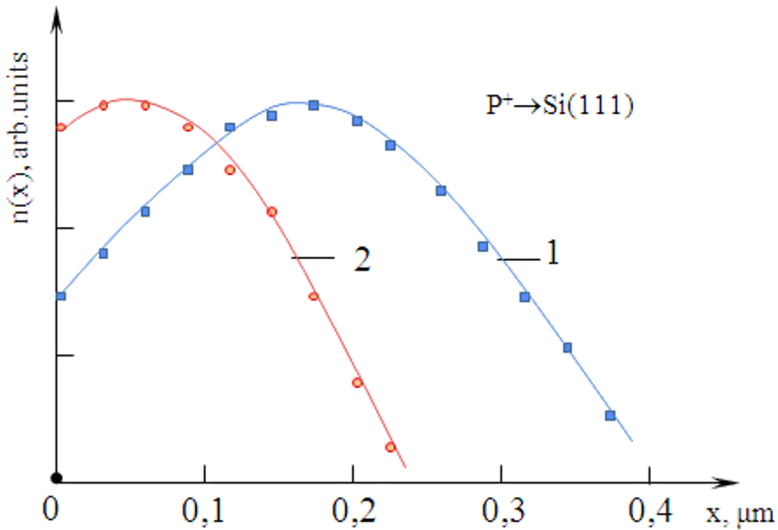


Fig. 4. Distribution profiles of phosphorus atoms over depth x , implanted into Si(111) with (1) energy $E_0 = 80 \text{ keV}$ and dose $D = 1.8 \cdot 10^{16} \text{ cm}^{-2}$ and (2) $E_0 = 20 \text{ keV}$ and $D = 1.8 \cdot 10^{15} \text{ cm}^{-2}$.

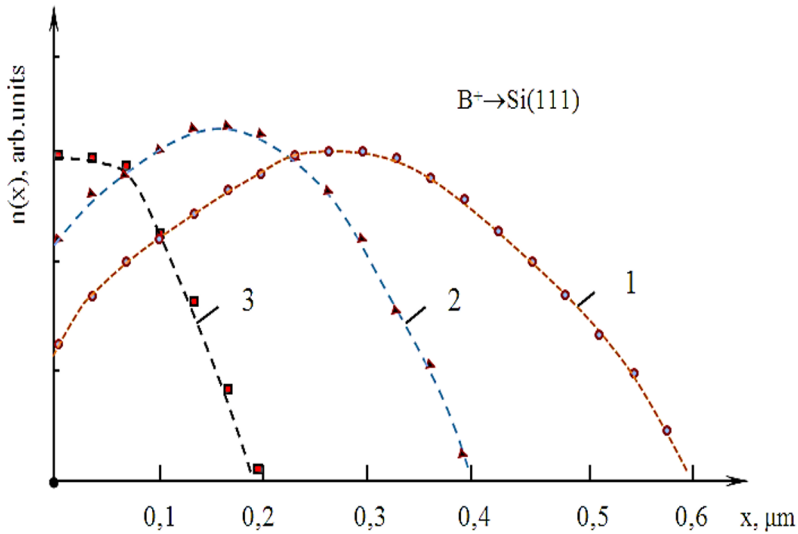


Fig. 5. Distribution profiles of boron atoms over depth x , implanted into Si(111) with (1) energy $E_0 = 80$ keV and dose $D = 0.9 \cdot 10^{16}$ cm $^{-2}$, (2) $E_0 = 25$ keV and $D = 3 \cdot 10^{15}$ cm $^{-2}$, and (3) $E_0 = 10$ keV and $D = 1.8 \cdot 10^{15}$ cm $^{-2}$.

Conducting annealing of defects (thermal heating or laser or infrared radiation) is obvious, along with a change in the distribution profiles of the P and B atoms, as well as their chemical state, should lead to a change in the electronic structure of the near-surface region of ion-implanted Si(111).

The chosen modes of ion implantation and subsequent annealing for electrical activation ensured a stepwise distribution of the atoms P and B and a sharp interface between the impurity and the base region of Si. Estimating the concentration of electrically active atoms by Auger electron spectroscopy (AES) shows that $N_p = 10^{21}$ cm $^{-3}$ and $N_B = 2 \cdot 10^{21}$ cm $^{-3}$. Similar results are obtained if, after each stage of ion doping, annealing is performed using pulsed laser radiation with an energy density of $W = 3$ J·cm $^{-2}$ (wavelength $\lambda = 1.06$ μm, pulse duration ~ 10 nanoseconds). That is, as a result of such ion implantation, it is possible to obtain a $p-i-n$ – structure with a high concentration of electrically active impurities and a sharp boundary between the $p-i$ and $i-n$ regions of Si. Note that a high concentration of carriers in the p and n regions of Si is also necessary to smooth the temperature dependence of the contact region of devices based on the $p-i-n$ junction. A fast electron diffraction (FED) study of the crystal structure of Si(111) surfaces after the above-mentioned ion implantation and subsequent annealing showed that both surfaces of the $p-i-n$ junction have a single crystal structure. It should be noted that the following methods are widely used to create thermosensitive structures based on the $p-n$ junction: 1) diffusion method, which consists in carrying out thermal diffusion of acceptor and donor type impurities into Si single crystals [18]; 2) epitaxial buildup of silicon layers from the gas phase in a medium enriched with acceptor or donor type [19]; 3) epitaxial - diffusion method, which consists in the combination of thermal diffusion of impurity with epitaxial growth of the p and n - regions [9].

Analysis of the capabilities of these methods for obtaining pn structures shows that in the first method, the process of thermal diffusion is carried out at sufficiently high temperatures, which leads to a blurring of the $p-i$ and $i-n$ – regions, as well as to their contamination with foreign impurities. This is reflected in the characteristics of the thermal

sensor: the linearity of the temperature dependence decreases, and the range of measured temperatures narrows.

The method of two-sided growing of epitaxial layers of *p*- and *n*- silicon allows one to obtain *p-i* and *i-n* transitions with a minimum concentration width, a smooth front edge, and a relatively uniform impurity distribution over the entire surface of the high-alloy layer [19]. However, diffusion of dopants from the epitaxial layers into the substrate is possible. The thickness of the diffusion layers is $\sim 1 \mu\text{m}$.

Using the epitaxial-diffusion method [20], combining the epitaxial growth processes with thermal diffusion of impurities from the gas phase. It is possible to slightly improve the characteristics of the devices compared to the above two methods. However, this method fails to obtain very high concentrations of active impurities, and the transition boundaries are not sharp enough, affecting the sensor's sensitivity and the range of measured temperatures. In addition, this method requires the use of expensive equipment for epitaxy. Thus obtained by us, *p-i-n* – the structure is a diode with hole conductivity of the base *i*-region is devoid of many of the disadvantages inherent in temperature sensors, obtained by the above traditional methods. To study the current-voltage characteristics of the *p-i-n* diode, metal contacts were deposited on both surfaces of the crystal. Metallization of the diode surface was carried out by vacuum deposition of Ti and Ni atoms installation under high vacuum conditions at the substrate temperature $T=600 \text{ K}$. And first, Ti and then Ni atoms were deposited. The thickness of the TiNi films on the surfaces of the *p-i-n* structure was $100\text{-}200 \text{ \AA}$. Volt-ampere characteristics of the *p-i-n* diode obtained by us, taken at different temperatures, have the traditional shape characteristic of diode structures, and the direct voltage drop across the *p-i-n* structure depends on the temperature of the diode (Fig. 6).

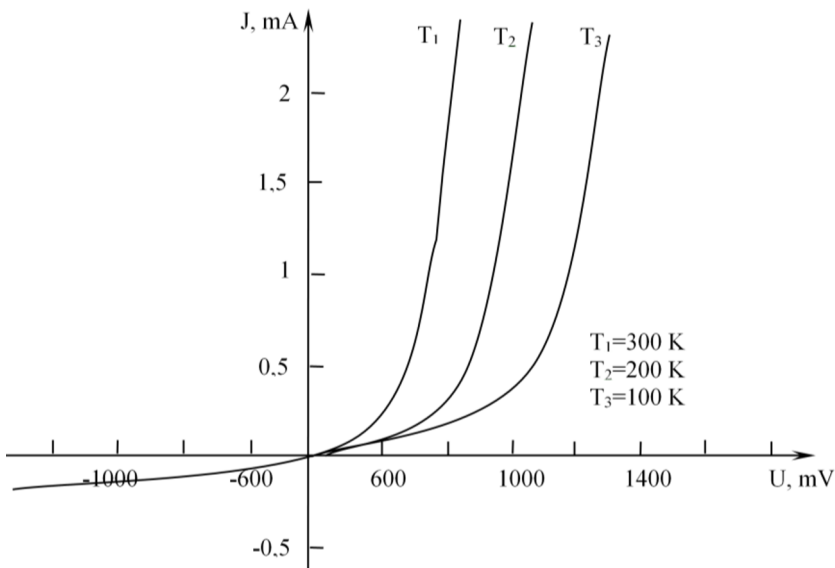


Fig. 6. Volt - current characteristics of *p-i-n* – diode, taken at different T : 100, 200, 300 K.

Studying the dependence of the direct voltage drop U_{dir} on temperature during the formation of a pin structure by implanting *P* and *B* ions into Si with a gradual decrease in the energy and dose of ions and conducting pulsed annealing showed that after the first stage of ion implantation, the dependence $U_{\text{dir}}=f(T)$ is not linear (curve 1). As a result of the second stage of ion implantation and annealing, the dependence $U_{\text{dir}}=f(T)$ becomes linear at

low temperatures of ~ 250 K. After the third stage of ion implantation and annealing, this dependence becomes linear throughout the entire temperature range (Fig. 7).

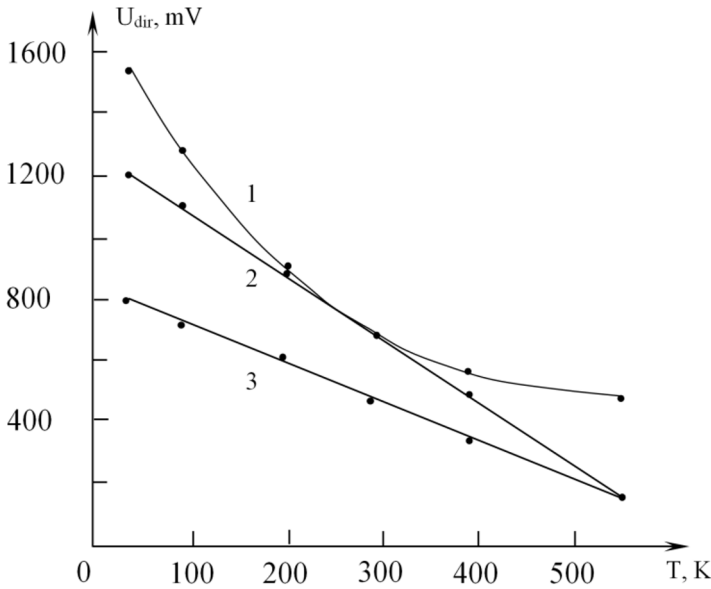


Fig. 7. Dependence of direct voltage drop on p-i-n – transition from heating temperature for Si(111) with specific resistance $\rho = 6000$ Ohm-cm (1) and 3000 Ohm-cm (2).

$U_{dir}=f(T)$ dependences are obtained by passing the current of the feeding $I_f=1$ mA through the p-i-n structure and connecting it to the circuit in the current stabilization mode ($I_f=const$). As seen from Fig. 7, the sensor performance also depends on the resistivity of the original silicon, i.e., determined by the processes in the base region of the p-i-n – diode. With a decrease in ρ of the original silicon, the sensitivity of the sensor decreases slightly. The picture of the temperature-sensitive element is shown in Fig. 8.

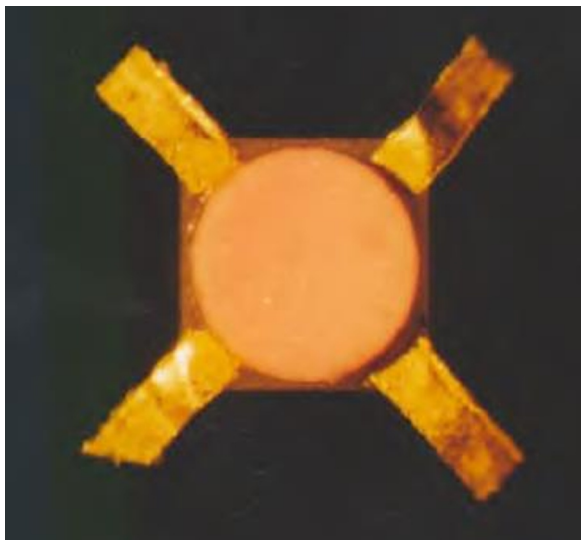


Fig. 8. Diode c p-i-n – junction.

4 Conclusions

It was shown that implantation of P and B ions in different directions of a Si(111) single crystal with a successive decrease in energy and radiation dose (for P^+ , first with energy $E_0=80$ keV and dose $D=1.8 \cdot 10^{16}$ cm⁻², and then with $E_0=20$ keV and $D=1.8 \cdot 10^{15}$ cm⁻², for B^+ - $E_0=80$ keV and $D=0.9 \cdot 10^{16}$ cm⁻², then $E_0=25$ keV and $D=3 \cdot 10^{15}$ cm⁻² and $E_0=10$ keV, $D=1.8 \cdot 10^{15}$ cm⁻²) and by conducting, after each implantation stage, pulsed IR or laser annealing with a wavelength $\lambda=1$ μ m, it is possible to create a uniform stepwise distribution of the atoms P and B and form $p-i-n$ – structures with sharp boundaries between $p-i$ and $i-n$ – transitions from to High concentration of electrically active atoms.

Thus, the above technological modes of ion implantation, pulsed IR, and laser annealing are optimal for obtaining a thermal sensor with the following parameters:

1) the range of measured temperatures: from 20 to 550 K. In the whole range, the dependence $U_{dir}=f(T)$ is linear;

2) temperature sensitivity is 2.3 mV·K⁻¹;

supply current from 100 μ A to 1 mA.

3) inertia does not exceed 10 ms.

It is established that the best characteristics are obtained when using Si samples with a thickness of 0.1 mm. With a decrease in the specific resistance of the initial silicon, the temperature sensitivity of the $p-i-n$ structure decreases.

References

1. Yuldashev Yu.Yu., Rysbaev A.S., Khujaniyozov J.B., Rakhimov A.M. Patent. №. IAP 04779, 10.10.2013.
2. Abdurakhmanov B.M., Aliev R. and et al. // Solar technology, 1998, № 4, p. 74-78.
3. B.M. Abdurakhmanov, L.O. Olimov and et al. // Solar technology, 1998, № 5, p. 78-83.
4. Abdurakhmanov B.M., Drachuk I.V., Sopen V.I., Akbarov Sh.K. // Uzbek journal of Physics, 2000, Vol. 2, № 1, p. 73-75.
5. Abdurakhmanov K.P., Vitman R.F., Guseva N.B., Kulikov G.S., Melikh B.T., Yusupova M.A. // FTP, 1996, № 3, p. 392.
6. Rysbaev A.S., Khujaniyozov J.B., Bekpulatov I.R., Rakhimov A.M., Pardaev O.R. Effect of Thermal and Laser Annealing on the Atom Distribution Profiles in Si(111) Implanted with P^+ and B^+ Ions. // Journal of surface investigation: X-ray, synchrotron and neutron techniques 2017, Vol. 11 № 2, p. 474-479.
7. Orekhov A.S. / Abstract of Ph.D. thesis, Moscow, 2017, 23 p.
8. Orekhov A.S., Kamilov T.S., Ibragimova B.V., Ivakin G.I., Klechkovskaya V.V. // Semiconductors, 2017, Vol. 51 № 6, pp. 706-709.
9. Karimov A.V., Mirzabaev M.A. Copyright certificate № 762253 from 02.16.1980.
10. Mirzabaev M.M., Rasulov K., Komilov A., Yusupova R.D. // Solar technology, 2000, № 1, p. 91.
11. Di Maria D.J. // J. Appl. Phys. 1981, Vol. 52, P. 7251.
12. Harstein A. and Fowler A.B. // J. Phys. 1975, Vol. 8, P. 249.
13. Bottoms W.R. and Gurerman D. // J. Vac. Scie and Technol. 1974, Vol.11, P. 965.
14. Ando T., Fowler A., Stern F. /Tomas J. Watson Reseach Center, New York, 1985 y., 415 p.

15. Rysbaev A.S., Khujaniyozov J.B., Rakhimov A.M., Bekpulatov I.R. / Patent № IAP 05720. 30.11.2018.
16. Oura K., Lifshits V.G., Saranin A.A., Zotov A.V., Katayama M. *Surface Science an Introdition.*/ Springer, 2006 y., pp. 105-114.
17. Rysbaev A.S., Khujaniyazov J.B., Rakhimov A.M., Bekpulatov I.R. // *Technical Physics*, 2014, Vol. 59, №. 10, pp. 1526–1530.
18. Andrey S. Orekhov, T.S. Kamilov, Anton S. Orekhov, N.A. Arkharova, E.V. Rakova, and V.V. Klechkovskaya. // *Nanotechnologies in Russia*, 2016, Vol. 11, Nos. 9–10, pp. 610–616.
19. Sladkov I.B. // *Abstract of the master's thesis*, 1971. 18 p.
20. Mirzabaev M.M., Rasulov K. / 1995. "Fan" ed. S.A. Azimov. pp. 101-135.